First Evidence of Cutaneous Remodelling Induced by Synchronized Radiofrequency Aided by High-Intensity Facial Muscle Stimulation: Porcine Animal Model

David E. Kent, MD,* Klaus Fritz, MD,†‡ Carmen Salavastru, MD,‡§ Rea Jarosova, MSc, PhD,‖ and Jan Bernardy, MVD, PhD‖

BACKGROUND The quality of one's facial appearance diminishes with aging as skin and underlying soft tissues deteriorate. Connective tissue and musculofascial degeneration leads to skin laxity and wrinkles developing.

OBJECTIVE To evaluate the effects of synchronized radiofrequency with high intensity facial stimulation technology on dermal collagen and elastin fibers in a porcine model.

MATERIALS AND METHODS Eight sows were divided into Active (N = 6) and Control (N = 2) groups. Synchronized radiofrequency and high intensity facial stimulation were delivered to the ventrolateral abdomen. The Active group received four 20-minute treatments, once a week. Control group was untreated. Skin biopsy sample were histologically analyzed for connective tissue changes pre- and post-treatment. Data were analyzed statistically ($\alpha = 0.05$).

RESULTS In the Active group: the collagen-occupied area at baseline was $1.12 \pm 0.09 \times 106\ \mu m^2$ and increased by +19.6% ($p < .001$) at 1-month and by +26.3% ($p < .001$) 2 months post-treatment; elastin-occupied area at baseline was $0.11 \pm 0.03 \times 106\ \mu m^2$ and increased by +75.9% ($p < .001$) at 1-month and +110.8% ($p < .001$) at 2-months follow-up. No significant changes ($p > .05$) found in the Control samples.

CONCLUSION Collagen and elastin fiber content increased significantly after treatments. Connective tissue in the treatment area was denser up to 2-months post-treatment.

Facial aging is a complex process involving changes in facial anatomy.[1] Various skin components, underlying muscle, and fibromuscular fascia are involved.[2–4] The fascial framework and the dermis consist of fibroelastic connective tissue primarily composed of collagen and elastin.[5,6] The muscles, fascia, and skin quality degenerate because of intrinsic and extrinsic factors, causing the skin to become slack and fragile.[7–9] Elastin and collagen content decline when there is an imbalance in protein turnover as the degradation of collagen is accelerated, whereas its synthesis is diminished. This lack of balance (dysregulation) causes further deterioration of connective tissue. There is a loss of tissue structural integrity and elasticity because of increased degradation of functional collagen and decreased collagen production. Fine lines (rhytids), wrinkles, and saggy skin are some signs of aging.[10–14]

*From the *Skin Care Physicians of Georgia, Macon, Georgia; †Dermatology and Laser Center, Landau in der Pfalz, Germany; ‡Carol Davila University, Bucharest, Romania; §Department of Dermatology, Colentina Clinical Hospital, Bucharest, Romania; ‖Veterinary Research Institute, Brno, Czechia*

The authors have indicated no significant interest with commercial supporters.

Address correspondence and reprint requests to: David E. Kent, MD, Skin Care Physicians of Georgia, 308 Coliseum Dr # 200, Macon, GA 31217, or e-mail: dekent@dsspc.com

Dermatol Surg 2024;00:1–4
http://dx.doi.org/10.1097/DSS.0000000000004028

Radiofrequency (RF) causes neocollagenesis in the skin at temperatures of 40 to 45°C.[15] Thermal energy destabilizes the collagen fiber.[16] This collagen structure disruption results in the stimulation of fibroblasts needed for increased neocollagenesis and neoelastogenesis.[17]

The HIFES modality aims to remodel and tone delicate facial muscles, counter the sagging appearance of skin, and improve the facial contour with increased volume.[18] To maximize the benefits of facial treatments, a novel device using synchronized RF with HIFES was developed. Combining these 2 different technologies targets superficial (dermal) and deep (muscle and fascia) tissue components. The simultaneous application of RF and HIFES technologies may be useful in improving facial appearance characterized by sagging, wrinkles, and rhytids.

This veterinary study aimed to evaluate the effects of synchronized radiofrequency and HIFES technology on porcine skin, particularly effects of the therapy on collagen and elastin fibers in the dermis, through a noninvasive hands-free applicator.

Materials and Methods

This veterinary study protocol was approved by the Ethics Committee for Animal Protection of the Ministry of Agriculture of the Czech Republic. Before the study, the animals underwent blood tests to assess their condition and health status. Animals were kept at ambient room temperature and fed a cereal diet. The study was conducted on 8 female large white pigs (*Sus scrofa* domesticus),

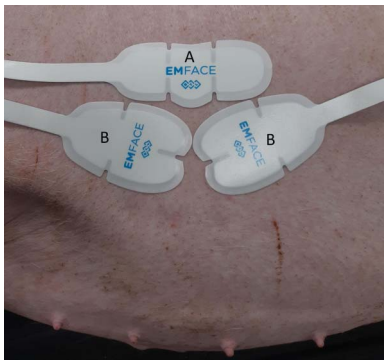

Figure 1. Illustrative set-up of the hands-free, self-adhesive device applicators on the ventrolateral abdomen of a sow that received active simultaneous RF and HIFES treatment. In human subjects, applicator A is intended for the forehead and B for the cheeks.

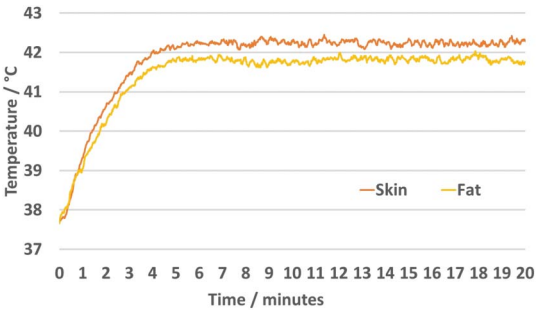

Figure 2. Thermoprobe measurement results during the treatment. The threshold temperature of approximately 40 to 42.5°C was reached in the dermis within the first 2 minutes and maintained in the range for the rest of the treatment time. The temperature in the fat was also monitored, showing about half a degree lower temperatures than the dermis.

weighing between 60 and 80 kg. There were 2 study groups, namely, the active group with 6 sows receiving simultaneous RF and HIFES therapy under general settings, and the control group with 2 untreated sows.

The synchronized RF and HIFES treatments were delivered with a study device (EMFACE, BTL Industries Inc, Boston, MA) through noninvasive self-adhesive electrode applicators placed on the ventrolateral part of the abdomen of the sows (Figure 1). The area covered by the electrode applicator had a diameter of 15 cm, and the treatment lasted 20 minutes at 100% power setting. The temperature in the dermis and subcutaneous fat layer was measured using a fiber optic temperature probe (LumaSense Flurotropic Thermometer) inserted into the tissue using an 18-G 1.5-inch injection needle. Treatment was done once per week for a total of 4 weeks. Treated sows were kept under full general anesthesia during the introduction to the surgical hall and the entire treatment phase, which lasted up to approximately 1 hour before awakening again.

Skin samples were collected by punch biopsy (6 mm diameter, Kruse Buster) from the treatment area (in the active group) and in the analogous anatomical area of the untreated control animals. Biopsies were obtained pretreatment (baseline) and post-treatment (1-month and 2-months follow-ups) in all animals including the control. After biopsy sampling, the wounds were dressed.

Histologic Analysis

The tissue samples from the punch biopsy were processed and sectioned in preparation for Orcein and Trichrome staining protocol. After staining, slides were mounted and observed. In total, 6 slices were prepared out of every biopsy sample.

Collagen

Masson's trichrome procedure was followed for collagen-specific staining. Collagen fibers were selectively stained and developed a green color. The stained samples were mounted to a microscopy slide.

Elastin

Visualization of elastin fibers was done with Orcein staining protocol. The elastin fibers were selectively stained and developed a brown-dark color.

The slides were observed and photographed using an automated slide scanning microscope (Hitachi Axio Scan.Z1, Carl Zeiss AG, Germany; 20×/0.8NA Plan-Apochromat objective) in a bright field. Quantitative analysis of collagen and elastin was performed with the Image J software based on semi-automatic segmentation in the Hue-Saturation-Brightness color system. The appropriate threshold differentiating the collagen and elastin fibers from the background was identified in the selected regions of interest (ROI = 1800 × 1,200 μm). After the collagen and elastin fibers were selected, their densities were expressed as the occupied area (square micrometers), which the fibers encompassed in the studied images' ROI.

Statistical analysis Student *t*-test and repeated measures analysis of variance test were performed with significance level set at $\alpha = 0.05$. Post-hoc Tukey honest significant test was conducted for multiple comparisons.

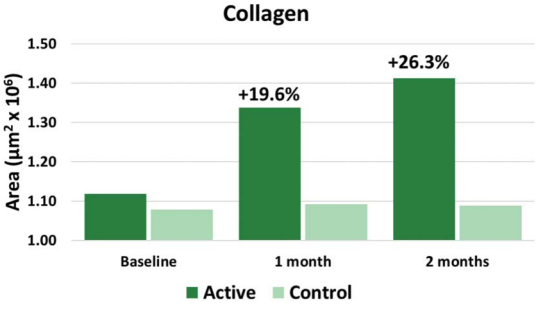

Figure 3. In the active group, the collagen fibers ($p < 0.001$) increased, occupying a greater area after 2 months follow-up compared to baseline. No significant change occurred in the control group.

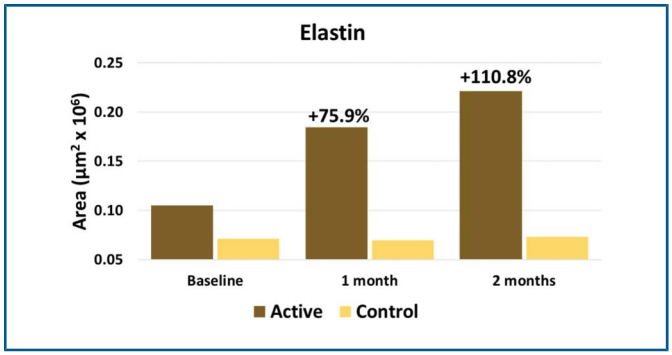

Figure 4. In the active group, the elastin fibers ($p < 0.001$) increased, occupying a greater area after 2 months follow-up compared to baseline. There was no significant change in the control group.

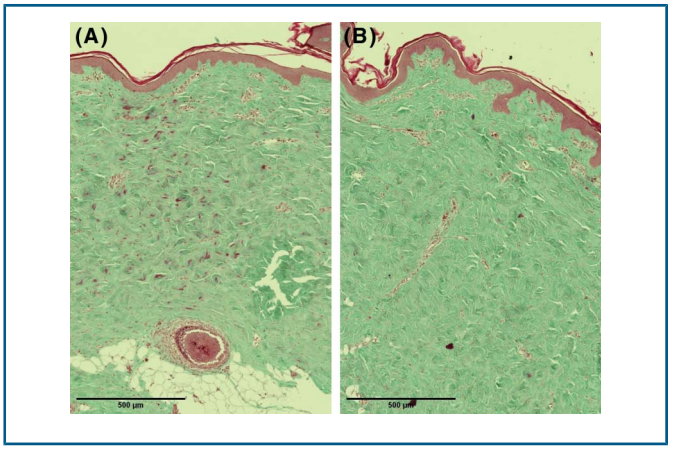

Figure 5. Bright-field visualization of collagen fibers stained by trichrome stain, active group sample. The collagen fibers appear in green color. In the slide on the right (2-months follow-up, B), the collagen fibers are noticeably denser, occupying a greater area when compared to the left (baseline, A).

Results

All the sows were in good health and condition before and during the study duration. The animals recovered from anesthesia without any complications. The dermal temperature was maintained slightly above 42°C, although not exceeding 42.5°C. The measurements in the fat layer showed a temperature elevation to approximately 41.9°C, elucidating the nature of the temperature gradient observed during the treatment (Figure 2). There were no side effects or adverse events related to the treatment.

Collagen

In the active group, the average area occupied by collagen was 1.12 ± 0.09 × 106 μm^2 at baseline. The average collagen-occupied area increased to 1.34 ± 0.08 × 106 μm^2 and 1.41 ± 0.07 × 106 μm^2 at the 2-month follow-up. Compared with baseline, in the active group, the average collagen amount increased ($p < .001$) at both post-treatment follow-ups. In the control group, there was no significant difference ($p > .05$) in collagen fibers, because the collagen content fluctuated in the range of 1.08 ± 0.04 to 1.09 ± 0.05 × 106 μm^2 throughout the whole study. There was a significant difference ($p < .001$) in the collagen-occupied sample area at both the 1-month (+19.6%) and 2-month (+26.3%) follow-ups (Figure 3) when comparing treated and control samples.

Elastin

In the active group, the mean elastin-occupied area at baseline was 0.11 ± 0.03 × 106 μm^2. At the 1-month follow-up, the average elastin amount was 0.19 ± 0.02 × 106 μm^2. At the 2-month follow-up, the area encompassed by elastin increased further to 0.22 ± 0.03 × 106 μm^2. Compared with baseline, the average elastin-occupied area increased at both follow-ups ($p < .001$). At both, the 1-month (+75.9%) and 2-month (+110.8%) follow-ups, the amount of elastin was significantly different ($p < .001$) comparing the active and control group (Figure 4). In the control group, there were no significant changes ($p > .05$) in elastin density at the follow-up points, elastin content ranged between 0.71 ± 0.04 × 106 to 0.73 ± 0.06 × 106 μm^2.

Exemplary samples of the collagen (Figure 5A,B) and elastin (Figure 6A,B) microscopic evaluation results of the active group are shown below.

Discussion

This study evaluated the effects of synchronized RF and HIFES on porcine skin. Histologic analysis of connective tissue structural proteins in the dermis showed a statistically significant increase in collagen and elastin content at 1 month and 2 months post-treatment. All the treated animals in the study recovered well after each treatment and did not experience any complications or adverse events.

Collagen production and remodeling are vital in tissue regeneration and may be beneficial to promote connective

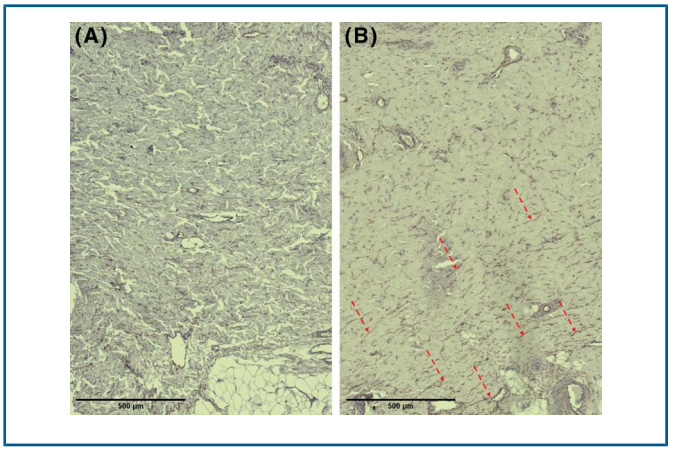

Figure 6. Bright-field visualization of elastin fibers stained by Orcein stain (active group sample). The baseline sample (left, A) has noticeably fewer elastin fibers, observed as dark/brown filaments (indicated by red arrows), than the 2-month follow-up (right, B). The surrounding collagen tissue (pale grey) also appears denser and better organized at 2 months post-treatment.

tissue fascia repair in the skin of the face. In this study, collagen content increased by +19.6% at 1 month and +26.3% at 2 months post-treatment follow-up. Elastin content increased by +75.9% at 1 month and +110.8% at 2 months after treatment, indicating that combined RF and HIFES enhanced expression of both structural proteins. The HIFES modality, in combination with RF, is intended for noninvasive improvement of skin tissue quality. Therefore, if confirmed in human subjects, this treatment method may be an alternative to current, invasive procedures aimed at improving facial appearance.[19–23]

To achieve a therapeutic effect on the skin, reaching the desired tissue temperature is key. Sustaining a lower, moderate therapeutic temperature between 40 and 45°C is essential for treatment effectiveness to circumvent cutaneous tissue necrosis and side effects because of overheating.[24] As shown in Figure 2, the dermal temperature measured via a thermal probe reached 40°C within the first 2 minutes from the start of the treatment and was maintained in the range 40 to 42.5°C for the duration of the treatment. This temperature is the target therapeutic range, which ensures treatment efficacy without affecting the underlying fat tissue, as intended during facial treatments. However, the effect on the fat should be a subject of further studies to fully rule out any alterations in response to the treatment.

The control group and temperature tracking were objective evaluation methods. Alternatively, immunofluorescence and scanning electron microscopy may be used for comprehensive connective and adipose tissue analysis. Gross examination of subcutaneous adipose tissue would expound the knowledge about the effects of sublipolytic temperatures on the underlying fat tissue structure in the treated area.[25,26]

Conclusion

The novel RF + HIFES technology for targeting facial skin, fascia, and muscles was investigated with a focus on the changes in the skin tissue using a porcine animal model. The study results showed that the procedure induces a denser network of collagen and elastin fibers in porcine skin after treatment with synchronized radiofrequency and HIFES observed through histologic analysis and skin temperature measurement. The enhanced collagen and elastin expression observed in this study may be beneficial for skin remodeling and revitalization if replicated in human subjects.

References

1. Swift A, Liew S, Weinkle S, Garcia JK, et al. The facial aging process from the "inside out". *Aesthet Surg J* 2021;41:1107–19.
2. Whitney ZB, Jain M, Zito PM. *Anatomy, Skin, Superficial Musculoaponeurotic System (SMAS) Fascia*. StatPearls Publishing; 2021. Available from: https://www.ncbi.nlm.nih.gov/books/NBK519014/. Accessed April 27, 2022.
3. Ganceviciene R, Liakou AI, Theodoridis A, Makrantonaki E, et al. Skin anti-aging strategies. *Dermatoendocrinol* 2012;4:308–19.
4. Okuda I, Yoshioka N, Shirakabe Y, Akita K. Basic analysis of facial ageing: the relationship between the superficial musculoaponeurotic system and age. *Exp Dermatol* 2019;28:38–42.
5. Robert L, Labat-Robert J, Robert AM. Physiology of skin aging. *Clin Plast Surg* 2012;39:1–8.
6. Pratt RL. Hyaluronan and the fascial frontier. *Int J Mol Sci* 2021;22: 6845.
7. Baumann L, Bernstein EF, Weiss AS, Bates D, et al. Clinical relevance of elastin in the structure and function of skin. *Aesthet Surg J Open Forum* 2021;3:ojab019.
8. Bonjorno AR, Gomes TB, Pereira MC, de Carvalho CM, et al. Radiofrequency therapy in esthetic dermatology: a review of clinical evidences. *J Cosmet Dermatol* 2020;19:278–81.
9. Kwan KR, Kolansky Z, Abittan BJ, Farberg AS, et al. Skin tightening. *Cutis* 2020;106:134–7;139;E1.
10. Yamauchi M, Taga Y, Hattori S, Shiiba M, et al. Analysis of collagen and elastin cross-links. *Methods Biol* 2018;143:115–32.
11. Uitto J, Li Q, Urban Z. The complexity of elastic fibre biogenesis in the skin—a perspective to the clinical heterogeneity of cutis laxa. *Exp Dermatol* 2013;22:88–92.
12. Naylor EC, Watson REB, Sherratt MJ. Molecular aspects of skin ageing. *Maturitas* 2011;69:249–56.
13. Fritz K, Bernardy J, Tiplica GS, Machovcova A. Efficacy of monopolar radiofrequency on skin collagen remodeling: a veterinary study. *Dermatol Ther* 2015;28:122–5.
14. Reilly DM, Lozano J. Skin collagen through the lifestages: importance for skin health and beauty. *Plast Aesthet Res* 2021;8:2.
15. Shoulders MD, Raines RT. Collagen structure and stability. *Annu Rev Biochem* 2009;78:929–58.
16. Wilczyński S, Stolecka-Warzecha A, Deda A, Koprowski R, et al. In vivo dynamic thermal imaging of skin radiofrequency treatment. *J Cosmet Dermatol* 2019;18:1307–16.
17. Kinney B, Bernardy J, Jarošová R. Novel technology for facial muscle stimulation combined with synchronized radiofrequency induces structural changes in muscle tissue: porcine histology study. *Aesthet Surg J* 2023;43:920–7.
18. Araújo ARd, Soares VPC, Silva FSda, Moreira TdS. Radiofrequency for the treatment of skin laxity: mith or truth. *Bras Dermatol* 2015;90: 707–21.
19. Nelson AA, Beynet D, Lask GP. A novel non-invasive radiofrequency dermal heating device for skin tightening of the face and neck. *J Cosmet Laser Ther* 2015;17:307–12.
20. Salvatore L, Gallo N, Natali ML, Terzi A, et al. Mimicking the hierarchical organization of natural collagen: toward the development of ideal scaffolding material for tissue regeneration. *Front Bioeng Biotechnol* 2021;9:644595.
21. Motosko CC, Khouri KS, Poudrier G, Sinno S, et al. Evaluating platelet-rich therapy for facial aesthetics and alopecia: a critical review of the literature. *Plast Reconstr Surg* 2018;141:1115–23.
22. MacGregor JL, Tanzi EL. Microfocused ultrasound for skin tightening. *Semin Cutan Med Surg* 2013;32:18–25.
23. Sadick NS, Nassar AH, Dorizas AS, Alexiades-Armenakas M. Bipolar and multipolar radiofrequency. *Dermatol Surg* 2014;40:S174–179.
24. Carruthers J, Fabi S, Weiss R. Monopolar radiofrequency for skin tightening: our experience and a review of the literature. *Dermatol Surg* 2014;40:S168–173.
25. Swindle MM, Makin A, Herron AJ, Clubb FJ, et al. Swine as models in biomedical research and toxicology testing. *Vet Pathol* 2012;49: 344–56.
26. Wilks BT, Evans EB, Howes A, Hopkins CM, et al. Quantifying cell-derived changes in collagen synthesis, alignment, and mechanics in a 3D connective tissue model. *Adv Sci* 2022;9:2103939.